DOI: 10.1002/zaac.201000227

Methane Storage in Prussian Blue Analogues and Related Porous Solids: Nature of the Involved Adsorption Forces

Blanca Zamora,[a] Jorge Roque,[a] Jorge Balmaseda,[b] and Edilso Reguera*[a,c]

Keywords: Methane storage; Adsorption; Porous solids; Prussian blue; Zeolite analogues

Abstract. Methane adsorption is possible through three types of interactions: (1) dispersive forces (van der Waals type); (2) polarization of its electron cloud by a positive charge center; (3) induced quadrupole moment by perturbation of the molecule electron cloud through the polarization interaction. This induced quadrupole moment is able to interact with the local electric field gradient. Porous Prussian blue analogues and related zeolite-like zinc hexacyanometallates appear to have unique features for the evaluation of the relative importance of these adsorption forces for the methane storage in molecular porous materials. Methane adsorption isotherms for $T_3[Co(CN)_6]_2$ (T = Mn, Co, Ni, Cu, Zn, Cd) and $Zn_3A_2[Fe(CN)_6]_2$ (A = Na, K, Rb, Cs) were recorded and interpreted. From the obtained adsorption data information on the relative contribution of both electrostatic and dispersive interactions to the adsorption forces was obtained.

Introduction

Methane is the main component of natural gas. It has the highest H/C ratio for a hydrocarbon and, in consequence, the minimum CO_2 production during the combustion reaction. In this reaction 55.48 kJ·g^{-1} of energy are liberated, which is above the value obtained from gasoline (47.5 kJ·g^{-1}). These two features and the great worldwide availability of methane-containing natural gas deposits have stimulated its application not only as energy bearer for homes and business but also in mobile technologies and as source for hydrogen production. Methane can also be obtained by decomposition of organic wastes. In order to address the development of appropriate methods for methane storage to be applied in mobile applications, the U.S. Department of Energy (DOE) has set the target of 180 V(STP)/V (STP = equivalent of methane per volume of adsorbent material storage system), under 35 bar and near ambient temperature. This target allows to obtain an energy density of adsorbed methane, which is similar to that of current compressed natural gas systems [1, 2]. Up to date, that target has been satisfied only for some activated carbon [1, 2] and metal-organic frameworks (MOFs) [3–5]. For some MOF compositions, the highest methane storage capacity, ≈ 230 V(STP)/V, 28 % above the DOE target, was reported [3]. Such behavior has been ascribed to the presence of a specific methane interaction with available open metal sites at the material cavities surface [4, 5]. The methane molecule can be adsorbed through both dispersive and electrostatic interactions. The electron cloud of this molecule has certain ability to be polarized by a charge center. Its polarizability constant (α) is 2.60 Å^3, above three times the value for H_2 (0.8023 Å^3), for instance [6].

Porous Prussian blue (PB) analogues and related zeolite-like zinc hexacyanometallates represent unique families of porous solids, where information on the relative contribution of both dispersive and electrostatic interactions to the adsorption forces for the methane molecule can be obtained. In this study two series of these families of porous materials where considered: $T_3[Co(CN)_6]_2$ with T = Mn, Co, Ni, Cu, Zn, Cd; and $Zn_3A_2[Fe(CN)_6]_2$ with A = Na, K, Rb, Cs. In the following these series will be labeled as T_3Co_2 and $Zn_3A_2Fe_2$, respectively. From the recorded methane adsorption data information on the nature of the prevailing adsorption forces was obtained. These two series of porous solids have been evaluated for hydrogen storage [7–14] but, to the best of our knowledge, this is the first study on the methane adsorption in their porous frameworks.

Results and Discussion

Characterization of the Samples to be Studied

Information on the crystal and electronic structures and thermal stability for the materials under consideration is available from previous studies [14, 15] and here only a summary of their features is provided. The PB analogues series crystallizes with a cubic unit cell, where the cell edge corresponds to the

* Prof. Dr. E. Reguera
E-Mail: ereguera@yahoo.com
[a] Centro de Investigación en Ciencia Aplicada y Tecnología Avanzada del IPN
Unidad Legaria
CICATA-Legaria
Legaria 694 Col. Irrigacion Del. M. Hidalgo
México City 11500, México
[b] Laboratorio de Polímeros
Instituto de Investigaciones en Materiales, UNAM
México City 11500, México
[c] Instituto de Ciencia y Tecnología de Materiales
Universidad de La Habana
La Habana, Cuba
Supporting information for this article is available on the WWW under **http://dx.doi.org/10.1002/zaac.201000227** or from the author.

Zeitschrift für anorganische und allgemeine Chemie ZAAC Journal of Inorganic and General Chemistry

T–N≡C–Co–C≡N–*T* chain length. The nature of the porous framework for this series is related to the existence of systematic vacancies for the building block, $[Co(CN)_6]$. At the surface of the generated cavities, *T* metal sites with an unsaturated coordination sphere, six per cavity, are found. In the as-synthesized material these available coordination sites are occupied by water molecules. The cavity filling is completed by additional water molecules stabilized by hydrogen bonding interactions with the coordinated ones. Both coordinated and weakly bonded water molecules evolve on moderate heating (below 370 K see Table 1) except for *T* = Ni without the material framework disrupting. For nickel, temperatures above 390 K are required to obtain an anhydrous solid (see Supporting Information). The dehydration process leads to a unit cell volume reduction of ca. 3 %. The obtained anhydrous porous solid then remains stable up to above 525 K. The exception in that sense corresponds to *T* = Zn. For this metal the material dehydration under heating is accompanied of a structural transition, from cubic to rhombohedral ($R\bar{3}c$ space group) [15]; in the following Zn_3Co_2–*R*.

Table 1. Cell edges, crystallite size, and temperature of dehydration for the two series of studied solids.

Compound	Cell edges /nm	Crystallite size /nm[a)]	Dehydration Temperature /K
Mn_3Co_2	1.0421(1)	68	365
Co_3Co_2	1.0220(1)	18	365
Ni_3Co_2	1.0162(1)	10	390
Cu_3Co_2	1.0062(1)	28	340
Zn_3Co_2	1.0263(1)	74	330
Cd_3Co_2	1.0591(1)	37	360
Zn_3Co_2–*R*	*a* = *b*: 1.2485(1), *c*: 3.2756(1)	–	[b)]
$Zn_3Na_2Fe_2$	*a* = *b*: 1.2479(1), *c*: 3.2906(3)	–	473
$Zn_3K_2Fe_2$	*a* = *b*: 1.2541(1), *c*: 3. 2158(1)	–	436
$Zn_3Rb_2Fe_2$	*a* = *b*: 1.2501(1), *c*: 3.2512 (1)	–	390
$Zn_3Cs_2Fe_2$	*a* = *b*: 1.2484(1), *c*: 3.2832(4)	–	370

a) The crystallite size was estimated only for the cubic phases.
b) Anhydrous solids.

The zeolite-like series, $Zn_3A_2[Fe(CN)_6]_2$, also crystallizes with the $R\bar{3}c$ rhombohedral unit cell, where the exchangeable metal (*A*) is found as hydrated species within the cavities system. This series can also be dehydrated under heating without the framework disrupting [14]. The temperature required to obtain an anhydrous solid depends on the involved *A* metal, particularly: Na: 473 K; K: 436 K; Rb: 390 K; Cs: 370 K. For a big ion like Cs^+ the water molecule remains far from the charge center and its removal is possible using relatively low thermal energy. The TG curves for the two considered series are available in Supporting Information. In Table 1 the cell edge values for the two series of hexacyanometallates are collected. For the PB analogues series the crystallite size depends on the involved *T* metals; it was found to be: Mn (68 nm), Co (18 nm), Ni (10 nm), Cu (28 nm), Zn (74 nm), Cd (37 nm) (see Table 1).

Porous Frameworks

For PB analogues series the porous framework is formed by cavities of ca. 8.5 Å diameter communicated by the interstitial spaces of ≈ 4 Å (Figure 1a). Such cavity size is enough to allow the methane molecule diffusion, which has a kinetic diameter of 3.8 Å [6]. The available free volume in the structure of this series depends on the distribution mode for the vacancies. To a totally random vacancy distribution neighboring cavities remain isolated, with the interstitial spaces as communication windows and the nominal free volume reaches its minimum value; it is 1/3 of the unit cell volume. Such vacancy distribution leads to a highly symmetric structure ($Fm\bar{3}m$ space group). In the anhydrous state the metal (*T*) remains coordinated to four nitrogen ends of CN groups, $T(NC)_4$ [15]. The opposite case corresponds to a system of ordered vacancies, where 1/2 of the unit cell volume remains unoccupied, with a crystal structure based on a primitive space group ($Pm\bar{3}m$). This structure contains two different sites for the metal *T*, $T(NC)_2$ and $T(NC)_5$, and it was observed for *T* = Cu [13].

The porous framework for the zeolite-like series appears as the assembling of MC_6 octahedra and ZnN_4 tetrahedra to form ellipsoidal cavities of about 12.5 × 9 × 8 Å, which are communicated by elliptical opening (windows) of ca. 4.5 Å (Figure 1b). The synthesis process really corresponds to the assembling of octahedral anionic blocks, $[M(CN)_6]^{n-}$, through Zn^{2+} cations, which link neighboring blocks at the nitrogen ends. The charge balancing is satisfied by the presence of an exchangeable alkali ion, A^+, located within the cavities. That ion is found close to the nitrogen ends at the cavity windows, where the framework has certain accumulation of negative charge [14]. Since in the structure there are two ions (A^+) per cavity and it has six windows, the structural sites for the metal *A* have statistical occupation. In order to minimize the electrostatic repulsion between ions within a given cavity, they must be located at opposite windows (maximum distance among them), and adopting a crossed configuration respect to the anions found within the neighboring cavities. For Zn_3Co_2–*R* the anhydrous solid is free of charge centers but its framework has certain charge accumulation close to the nitrogen ends, which is responsible for the presence of a weak electric field gradient in the windows region, sufficient to favor the H_2 adsorption in this material [14]. The two series of materials under study are nanoporous solids with an equivalent BET surface in the 570 (Ni) to 870 (Mn) $m^2 \cdot g^{-1}$ range for PB analogues [7] and of about 570 $m^2 \cdot g^{-1}$ for the zeolite-like series [16].

Interactions Involved in the Methane Molecule Adsorption

The methane adsorption is possible through three different interactions: (1) dispersive forces (van der Waals type) related to appearance of instantaneous dipole and quadrupole moments by fluctuations of the electron cloud of both, adsorbent, and adsorbate; (2) polarization of its electron cloud by a positive charge center and; (3) the induced quadrupole moment interaction with the local electric field gradient. When the molecule electron cloud is polarized an induced quadrupole mo-

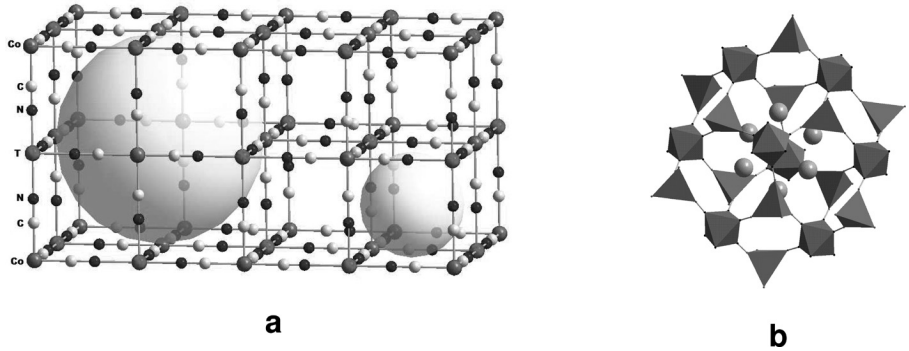

Figure 1. Porous framework of: a) Prussian blue analogues, the relatively large cavities due to the $[Co(CN)_6]$ vacancies (larger sphere) remain communicated by the interstitial spaces (smaller sphere). b) Zeolite-like zinc hexacyanometallates formed by ellipsoidal cavities communicated by elliptical windows. The exchangeable metal (A^+, small sphere) is found within the cavities, close to the windows.

ment appears. These three interactions have a strong dependence on the distance (r) between the interacting species, solid surface, and the guest molecule. The dispersive interactions are short distance forces, which depend on r^{-6} and of the amount of involved electrons; the contribution of the polarization force to the adsorption energy (E) depends on the strength of the local electric filed ($\boldsymbol{E}$) according to $E = (\alpha/2)|\boldsymbol{E}|^2$ and, in consequence, depends on r^{-4}; and the energy contribution when the induced quadrupole moment ($\boldsymbol{Q}$) interacts with the local electric field gradient ($\nabla\boldsymbol{E}$) is given by $E = -(1/3)\boldsymbol{Q}\cdot\nabla\boldsymbol{E}$ and depends on r^{-3}. These attractive interactions are compensated by the repulsive forces due to the electron clouds overlapping, exchange interaction, which depend on r^{-12}. Both polarization and quadrupole interactions are of electrostatic nature and appear together. In carbon base materials and MOF type frameworks free of charge centers, for instance, only dispersive forces contribute to the adsorption potential but, for zeolite with exchangeable metals within the cavities the two types of interactions, dispersive and electrostatic, are present.

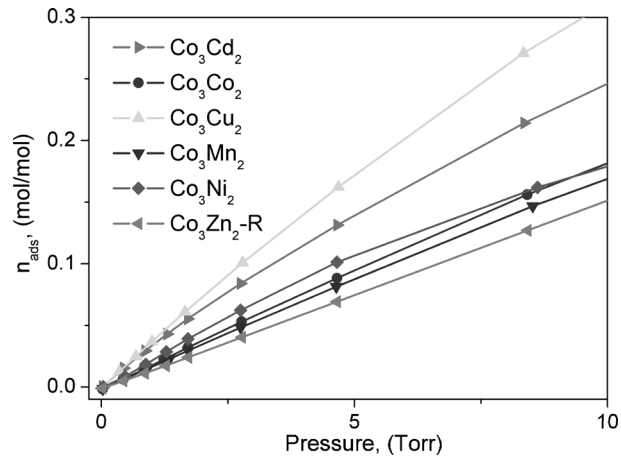

Figure 2. Low pressure region of the methane adsorption isotherms at 192 K in the PB analogues series. The strength for the adsorption interaction follows the order Cu > Cd > Ni > Co > Mn > Zn.

Methane Adsorption Isotherms

Figure 2 shows the low pressure region for the methane adsorption isotherms in PB analogues series. In that region the isotherms show a linear dependence on the pressure and according to the Henry's law their slope can be taken as sensor for the strength of the host-guest interaction. From this criterion, the strength for the methane-surface interaction follows the order Cu > Cd > Ni > Co > Mn. This order is quite different of that obtained for the metal polarizing power estimated from the dehydration temperature for this series, which is Ni > Mn > Co > Cd > Cu (see Supporting Information). Such behavior suggests that for this series the adsorption forces for methane are dominated by dispersive type interactions. With the exception of copper, the observed order for the adsorption potential follows the order of the metal (T) atomic number (Z); that is, of the amount of electrons found on the metal atoms. Such dependence supports the hypothesis that for this series the adsorption forces are dominated by dispersive type interactions.

The unique behavior observed for T = Cu can be ascribed to two factors: (a) the crystal structure, which contains two well defined structural sites for the copper atom, able to interact with the methane molecule; (b) the relatively high electron density on the copper atom, $Cu^{(2-\delta)+}$. The copper(2+) atom has a certain trend to receive electrons in its 3d hole in order to reach an electronic configuration close to $3d^{10}$. This trend is complemented by the ability of the CN group in PB analogues to donate electrons from its 5σ orbital, which has certain *anti*-bonding character [11]. These cooperative effects lead to an accumulation of electron density on the copper atom, contributing to a stronger dispersive interaction with guest molecules. The lowest isotherm slope, the weakest host-guest interaction was observed for T = Zn, where the metal has saturated its coordination sphere and the CN groups impede the access of the methane molecule to the metal environment. In summary, the observed order for the host-guest interaction strength, Cu > Cd > Ni > Co > Mn > Zn (Figure 2), finds explanation in the dispersive type interactions.

Figure 3 shows the methane adsorption isotherms up to 7600 Torr (10 bar) of pressure. The maximum amount of

Zeitschrift für anorganische und allgemeine Chemie ZAAC Journal of Inorganic and General Chemistry

methane molecules adsorbed in excess is similar for Mn, Co, Zn, and Cd. No large difference is expected for the cavity volume within these four metals. For the rhombohedral phase of zinc (Zn_3Co_2–*R*) the available free volume is about 90 % the value observed for the cubic phase [15]. The positive deviation observed for copper was ascribed to a non-random vacancy distribution, which leads to a greater cavity volume. The relatively low adsorption capacity found for nickel was interpreted as related to the low thermal stability for nickel PB analogue. For this metal the smaller crystallite size is obtained (10 nm) accompanied by the highest heating temperature required to obtain an anhydrous solid, > 120 °C (see Supporting Information). These two factors could be contributing to partial sample decomposition, a behavior already observed for this PB analogue [15].

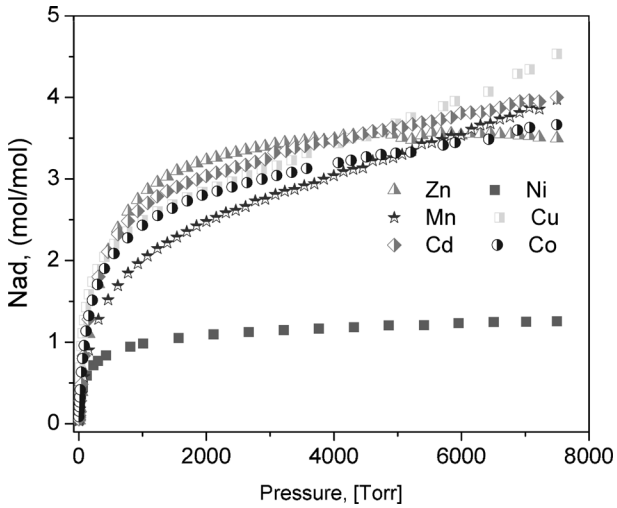

Figure 3. Methane adsorption isotherms at 192 K in the PB analogues series up to 7600 Torr (10 bar).

According to maximum CH_4 excess adsorption, within a cavity close to four molecules are accumulated. Considering that the adsorption experiment is carried out just above the critical temperature for methane, its maximum density within the cavity must be close to 0.43 g·cm^{-3}; which is the density value for liquid methane. From this density value the volume occupies by four CH_4 molecules results ≈ 250 Å^3, below the cavity volume estimated for PB analogues, which is close to 500 Å^3 considering its maximum hydration degree of 15 water molecules per cavity and a water density of 1 g·cm^{-3}. It seems the cavity volume for PB analogues is only partially occupied by methane. Of course, maximum estimated adsorption for the materials as a whole remains below the established target for methane storage in porous solids, 180 V(STP)/V, an expected behavior related to the nature of the considered porous solids. PB analogues involve relatively heavy metals.

Figure 4 shows the recorded isotherms for the zeolite like series, $Zn_3A_2Fe_2$ and Zn_3Co_2–*R*. For $A = Na^+$ and K^+, the material free volume results inaccessible to the methane molecule. These are the smallest cations within the considered alkali metals and, in consequence, with the smaller distance between the framework and the charge center. This leads to the strongest metal-framework interaction and probably to the lowest metal mobility during the adsorption process. This could explain the pore inaccessibility for methane in the presence of these two metals, since they are located close to the cavity windows. An alternative explanation can be given according to a strong polarization interaction between these two metals and the methane molecule, limiting the adsorbate diffusion through the porous framework. For the H_2 adsorption with *A* = Na, an analogous behavior was reported [14] but not for potassium. Compared with methane, hydrogen has a lesser polarizability constant (α), 0.8023 versus 2.60 Å^3 [6] and for potassium the strength of such interaction could be insufficient to avoid the hydrogen molecule diffusion. However, for CH_4 the polarizing power of the potassium ion could be sufficient to limit the adsorbate diffusion and the cavity filling.

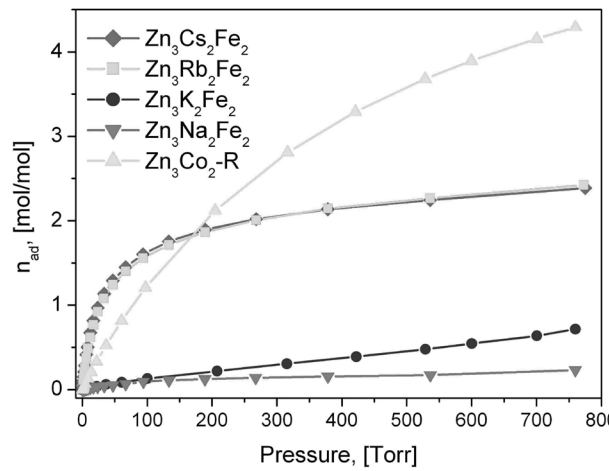

Figure 4. Methane adsorption isotherms at 192 K in the zinc zeolite-like series up to 760 Torr (1 bar). For *A* = Na and K, the porous framework is inaccessible to the methane molecule.

Such behavior cannot be attributed to the ion size properly, because for $A = Rb^+$ and Cs^+, greater size ions, the porous framework becomes accessible to the methane molecule (Figure 4). In the presence of these two metals the host-guest interaction for the methane molecule is particularly strong, at least compared with the behavior observed for the analogue free of exchangeable metal, Zn_3Co_2–*R* (Figure 4). For these two metals (Rb, Cs) the isotherm slope at low pressure values is quite pronounced. This corresponds to a strong host-guest interaction. To that strong interaction the two types of adsorption forces, dispersive and electrostatic, could be contributing. These metals occupy a relatively large fraction of the cavity volume increasing the methane molecule confinement within the cavity favoring a stronger dispersive interaction which is added to the electrostatic forces. For Zn_3Co_2–*R* the electrostatic contribution is probably negligible and the adsorption forces are dominated by van der Waals type interactions. The isotherm slope at low pressure for this material is significantly smaller than that observed when an alkali metal is present.

Conclusions

The study of the methane adsorption in porous PB analogues and related zeolite-like hexacyanometallates(II) sheds light on

the nature of the adsorption forces that are present during the interaction of this molecule with transition and alkali metals within the porous framework. Transition metal atoms are regions with a high electron density and their presence at the cavities surface favors the appearance of strong instantaneous dipole and quadrupole moments by fluctuations of the involved electron clouds, and of strong dispersive adsorption forces. The study of a homologous series containing different metals of open coordination sphere, like PB analogues, provides conclusive evidence on the nature of the prevailing adsorption forces for the methane molecule in that type of porous solids; the adsorption forces are dominated by dispersive interactions. For the zeolite-like series, the electrostatic forces contribution to the methane adsorption cannot be ignored particularly in the presence of ions of relatively small size, like Na^+ and K^+. Compared with H_2, for instance, the methane molecule has a relatively high polarizability constant, and the electrostatic interaction could be sufficient to impede the adsorbate diffusion through narrow channels and windows.

Experimental Section

The preparation of the materials in study has already been reported [14, 15]. The procedure can be summarized as follow: Aqueous solutions of the corresponding complex anion alkaline salts, $K_3[Co(CN)_6]$ or $K_4[Fe(CN)_6]$, were mixed, whilst stirring, with a solution of the involved metals (*T*) and the formed precipitates were aged within the mother liqueur for at least two days. The solid was separated by filtration (or centrifugation), washed several times with distilled water, and finally air dried until it had constant weight. Its nature as a metal hexacyanometallate was tested by infrared (IR) spectroscopy and the formula unit was established from chemical analyses. The structural characterization of the obtained material was carried from X-ray diffraction (XRD) data. The materials behavior on heating and the dehydration temperature were evaluated from thermogravimetric (TG) curves. For PB analogues series the crystallite size was calculated from the XRD peak width at half height using the Scherrer formula [17]. In Table 1 the main structural features for the two series of materials are summarized.

The methane adsorption isotherms were recorded at 192 *K*, which is slightly above the critical temperature of this adsorbate (190.4 K), using a cryogenic bath prepared mixing ethanol and CO_2 ice. ASAP 2020 and 2050 analyzers (from Micromeritic) were used, in order to obtain adsorption data in the 0.01–760 and 3–7600 Torr pressure ranges, respectively. Ultra high purity (99.999 %) methane was used as adsorbate. Sample tubes of known weight were loaded with ≈ 50 mg of sample and sealed using TranSeal. Previous to the adsorption experiment the samples were dehydrated in the ASAP activation port at the temperature indicated by the TG curve until to obtain a stable outgas rate below 1 μHg. For the zeolite-like series the dehydration temperature was, in absolute units (in K): Na: 473; K: 436; Rb: 390; Cs: 370. PB analogues series was also dehydrated under heating and moderate vacuum (10^{-1} Torr.) at the following temperatures (in K): Mn (350), Co (350), Ni (390), Cu (330), Zn (330), Cd (340). The degassed sample and sample tube were weighed and afterwards transferred back to the analyzer with the TranSeal preventing exposure of the sample to air. After volume measurement with helium the degassing was continued for 24 h in the sample port.

Acknowledgement

The partial support from *ICyTDF PIFUTP08-158* and *CUDI-CONACyT* projects is acknowledged.

References

[1] T. Burchell, M. Rogers, *SAE. Technol. Pap. Ser.* **2000**, 2001–2205.
[2] A. Celzard, V. Fierro, *Energy Fuels* **2005**, *19*, 573–583.
[3] S. Ma, D. Sun, J. M. Simmons, C. D. Collier, D. Yuan, H.-C. Zhou, *J. Am. Chem. Soc.* **2008**, *130*, 1012–1016.
[4] H. Wu, W. Zhou, T. Yildirim, *J. Phys. Chem. C* **2009**, *113*, 3029–3035.
[5] H. Wu, W. Zhou, T. Yildirim, *J. Am. Chem. Soc.* **2009**, *131*, 4995–5000.
[6] *CRC Handbook of Chemistry and Physics* (Ed.: D. R. Lide), 84th ed., CRC Press, Fl., USA, **2003–2004**.
[7] S. S. Kaye, J. R. Long, *J. Am. Chem. Soc.* **2005**, *127*, 6506–6507.
[8] K. W. Chapman, P. D. Southon, C. L. Weeks, C. J. Kepert, *Chem. Commun.* **2005**, 3322–3324.
[9] S. S. Kaye, J. R. Long, *Catal. Today* **2007**, *120*, 311–316.
[10] S. Natesakhawat, J. T. Culp, C. Matranga, B. Bockrath, *J. Phys. Chem. C* **2007**, *111*, 1055–1060.
[11] L. Reguera, C. P. Krap, J. Balmaseda, E. Reguera, *J. Phys. Chem. C* **2008**, *112*, 15893–15899.
[12] C. P. Krap, J. Balmaseda, L. F. del Castillo, B. Zamora, E. Reguera, *Energy Fuels* **2010**, *24*, 581–589.
[13] J. Jimenez-Gallegos, J. Rodríguez-Hernández, H. Yee-Madeira, E. Reguera, *J. Phys. Chem. C* **2010**, *114*, 5043–5048.
[14] L. Reguera, J. Balmaseda, L. F. del Castillo, E. Reguera, *J. Phys. Chem. C* **2008**, *112*, 5589–5597.
[15] J. Roque, E. Reguera, J. Balmaseda, J. Rodríguez-Hernández, L. Reguera, L. F. del Castillo, *Microporous Mesoporous Mater.* **2007**, *103*, 57–71.
[16] S. S. Kaye, J. R. Long, *Chem. Commun.* **2007**, 4486–4488.
[17] A. Guinier, *X-ray Diffraction*; Dover Publications: Mineola, NY, **1994**.

Received: June 1, 2010
Published Online: August 25, 2010

